Journal of Applied Physics

Temperature dependent magnetoelectric (ME) response in press-fit FeNi/PZT/Ni self-biased ring composite

Cite as: J. Appl. Phys. **126**, 094102 (2019); https://doi.org/10.1063/1.5108708
Submitted: 01 May 2019 . Accepted: 18 August 2019 . Published Online: 06 September 2019

Amritesh Kumar, and A. Arockiarajan

Journal of Applied Physics ARTICLE scitation.org/journal/jap

Temperature dependent magnetoelectric (ME) response in press-fit FeNi/PZT/Ni self-biased ring composite

Cite as: J. Appl. Phys. **126**, 094102 (2019); doi: 10.1063/1.5108708
Submitted: 1 May 2019 · Accepted: 18 August 2019 ·
Published Online: 6 September 2019

Amritesh Kumar and A. Arockiarajan[a)]

AFFILIATIONS

Department of Applied Mechanics, Indian Institute of Technology Madras, Chennai 600036, India

[a)]**Electronic mail:** aarajan@iitm.ac.in

ABSTRACT

Magnetoelectric (ME) composites exhibit the magnetoelectric effect, which is a coupling phenomenon resulting from the interaction between the magnetostrictive and piezoelectric phases. This makes ME composites useful as multifunctional devices in a variety of applications. In this work, a press-fit epoxy-free nested ring structured ME composite has been fabricated, in which nickel and FeNi form the magnetostrictive phase and PZT-5A constitutes the piezoelectric phase. To conduct a comparative study, epoxy bonded conventional bilayered and trilayered ME composites of the same material constituents and similar volume fractions have also been made. Magnetostriction measurements are done on individual magnetostrictive materials at varying temperatures in longitudinal and transverse directions. Measurement of the ME coefficient is done on all the prepared composites and their relative response at elevated temperatures is presented. Self-biased behavior of the ME composites resulting out of the applied prestress is also captured. A 2D hysteretic model including the temperature and prestress effects that can capture the behavior of epoxy-free ring composites has also been formulated. The results from the model are in agreement with the experimental results at all the temperatures. The obtained experimental results highlight the suitability of epoxy-free ring composites to be used in high temperature microdevices.

I. INTRODUCTION

Multiferroics are the materials that possess two or more ferroic orders (ferroelectric, ferromagnetic, and ferroelastic), the coupling interaction between which leads to product properties. The magnetoelectric (ME) effect is one such property that arises out of the coupling interaction between ferroelectric and ferromagnetic orders. The ME effect is the emergence of the electric polarization **P** on the application of a magnetic field **H** (direct ME effect) or the emergence of the magnetization **M** on the application of an electric field **E** (indirect ME effect).[1] Certain single phase materials show the ME effect as an innate response at low temperatures but a single phase material depicting significant coupling at room temperature is yet to be found. This restricts their applications for practical purposes. This has stimulated researchers to develop multiphase materials like magneto-electric composites. ME composites being multifunctional devices find a wide variety of applications in the form of transducers, sensors, actuators, and energy harvesters[2–5] along with recent biomedical applications.[6] Since the ME effect arises due to strain-mediated coupling, the efficiency of strain transfer from the magnetostrictive material to the piezoelectric material is crucial. The degree of ME effect observed is captured by the introduction of a magneto-electric coefficient often abbreviated as α. Mathematically, the ME coefficient for direct ME effect is given as $\alpha = \partial P/\partial H$, i.e., change in electric polarization **P** per unit change in magnetic field **H**. The major part of the research in this field deals with the observation and optimization of this ME coefficient. The three broad configurations of bulk ME composites under interest have been 0–3 particulate composite, 1–3 rod composite and 2–2 laminate composite, of which 2–2 laminate composites have been shown to display a giant ME coefficient.[7,8]

Though significant values of the ME coefficient have been obtained from layered composites, the need for a bias field to obtain the ME effect poses a limitation on their use in microdevices. This has led researchers to explore ME composites that could show the ME effect on excitation only by a small ac field (even in

the absence of bias field), which is termed as self-biased behavior. Self-biased behavior was seen in functionally graded ferromagnetic Ni-Metglas/PZT composite,[9] $Ni_{1-x}Zn_xFe_2O_4$ (NZFO)/*PZT* composite,[10] Sm doped ferrite $Ni_{1-x}Zn_xSm_{0.02}Fe_{1.98}O_4$/Pb(Zr, Ti)$O_3$ composite,[11] and SFO/Metglas/PZT.[12] Self-biased character obtained by the Ni/PMT composite marked the development of a single phased ferromagnetic material composed (unlike functionally graded ferromagnetic materials) self-biased ME composite.[13] In the later developments, such behavior was also seen in two-phased $SmFe_2$/*PZT*,[14] trilayered $SmFe_2$/*PZT*/$SmFe_2$,[15] NKNLS-NZF/Ni, and NKNLS-NZF/Ni/NKNLS-NZF composites.[16] All the above works involved the use of layered composite with different layers being attached by means of an epoxy material. Though some works have focused on the interface effects in ME composites,[17,18] but consistent efforts have been made to prepare epoxy-free ME composites. In order to obtain a better strain-mediated coupling behavior, an attempt to fabricate an epoxy-free self-biased ME composite was done by making NCZF/PMN-PT/NCZF layered composite prepared by the cofiring method.[19] Though this method provided advantages like bulk manufacturing and low cost production, this also posed certain problems in the form of mismatch of thermal expansion and different expansion rates. Pan *et al.* fabricated epoxy-free cylindrical Ni/PZT bilayered and Ni/PZT/Ni trilayered composites by the electrodeposition method.[20,21] A better response as compared to layered composites was reported but no self-biased behavior was obtained. Jing *et al.* prepared FeNi/PZT/Ni three phased press-fit embedded structured ME composite which apart from being epoxy-free also showed self-biased behavior.[22] To enhance the flexibility of application of ME composites, their performance at elevated temperatures becomes crucial. A survey of the plethora of the research work conducted in this regard reveals the absence of any temperature dependent study on the performance of such self-biased composites.

Delving into the modeling aspect, Carman and Mitrovic[23] first presented a 1D constitutive model for a magnetostrictive material including the effects of prestress. The model was compared with the experimental values of Terfenol-D[24] and could predict the behavior at lower fields but was unable to capture the saturation behavior. Later, efforts were made to combine the constitutive relations obtained from phenomenological and micromechanical approaches and model the behavior of 1–3 magnetostrictive composite based on a concentric cylinder model.[25] This 2D model could predict the magnetostrictive behavior by taking into account the prestress but showed the same level of saturation for any given prestress. Further, three constitutive models in the form of SS (Standard Square) model, HT (Hyperbolic Tangent) model, and DDS (Density of Domain Switching) model were proposed.[26] The SS model could not predict the magnetostrictive behavior apart from lower fields while the HT model and the DDS model overpredicted and underpredicted the saturation behavior, respectively. Zheng-Liu gave a classical model by splitting the strain caused due to prestress into a linear and a nonlinear part.[27] For the simplification of the model, the nonlinear part was linearized by the introduction of a flexibility tensor with the limitation of application to low prestress values. The model showed good adherence to the experimental results with the stated limitation. This limitation was revoked in a revised 1D model[28] in which the nonlinear part of the strain occurring due to prestress was accounted by assuming a hyperbolic tangent function. This 1D model could predict the magnetostrictive behavior for any applied prestress at any field. This 1D model was further extended to incorporate the temperature effects by introducing the variation of saturation magnetization with temperature.[29] The model showed good results for Terfenol-D rods at temperatures of 20 °C and 70 °C. A similar 1D model as for giant magnetostrictive material was also developed for soft ferromagnetic materials without including the temperature effects.[30]

Further developments led to a 1D hysteretic model[31] for magnetostrictive material wherein the total strain and magnetic field strength were decomposed into reversible and irreversible parts. Thereafter, analogous to the plasticity theory, the irreversible quantities served as the internal variables for the model. The model captured the hysteretic behavior to a great extent for Terfenol-D. An even more sophisticated 1D hysteretic model[32] taking into account the temperature and prestress effects was presented by incorporating the eddy current losses effects. The model calculated the effective field reaching the magnetostrictive sample and predicted close to accurate results for 1D Terfenol-D rods. Later, a 1D anhysteretic model[33] was developed by using the Jiles strain-magnetization relation. The total field was calculated by taking into account the temperature and prestress effects and the model predicted acceptable results at room temperature but showed major deviations at higher temperatures. Zhang *et al.*[34] proposed a different nonlinear function to approximate the nonlinear part of the strain coming from prestress. In this model, a different function in the form of $f(x) = (2/\pi)\arctan(x)$ was used in place of conventionally used Langevin or Hyperbolic tangent function. Along with closely matching with the experimental results, this model also overcame the limitation of using two constitutive models for compressive and tensile stress posed by the classical Zheng-Liu model. In the recent development, a 1D hysteretic model[35] including the temperature and prestress effects incorporating the eddy current loss effect was given to predict the behavior of the magnetostrictive material at static and dynamic frequency. The model result showed very good agreement with the experimental results. A finite element approach to capture the ME response of the layered Terfenol-D/PZT has been done and the results were found to be reasonably agreeable.[36] A vivid exploration of research in this field reveals that most of the developed models are one dimensional. Thus, there is absence of a single 2D hysteretic model that captures the temperature and prestress effects.

In this work, epoxy-free press-fit nested ring structured self-biased ME composite along with conventional epoxy bonded bilayered and trilayered ME composite have been fabricated. Experiments have been conducted at varying temperatures to find the temperature dependence of magnetostriction of individual magnetostrictive materials and the ME coefficient of the prepared ME composites of different configurations. A comparative study of the performance of the epoxy-free ring composite with respect to the epoxy bonded composites at elevated temperatures has been done. A 2D thermodynamically consistent hysteretic phenomenological composite model taking into account the effects of temperature and prestress to predict the behavior of the ring composite at elevated temperatures has been formulated. The derived constitutive relation encapsulates the nonlinear behavior of the magnetostrictive phase,

whereas for piezoelectric material, linear behavior has been considered. The temperature dependent self-biased behavior has been accounted by the introduction of appropriate material parameters.

II. EXPERIMENTAL DESCRIPTION

Experiments are conducted to understand the response of the epoxy-free ring structured ME composite under varying magnetic fields at elevated temperatures. Subsection II A describes the setup used for magnetostriction measurement of the individual constituent of the ME sample. Subsection II B highlights the sample preparation process. Subsection II C provides the detailed description of the measurement of the magnetoelectric coefficient (α_{ME}). Also, since this work aims to do a comparative study of the performance of epoxy-free composites as opposed to conventional epoxy bonded layered composites, a brief idea about the preparation and testing of epoxy bonded layered composites is also presented.

A. Magnetostriction measurement

In order to study and understand the behavior of the ME composites, magnetostriction measurements have been done on individual magnetostrictive components (nickel and FeNi). The experimental setup employed for this measurement has been shown in Fig. 1(a). For the purpose of clarity, a schematic of the setup has also been presented in Fig. 1(b). An electromagnet (GMW5403) having pole diameter of 36 mm is used to provide the magnetic field. The electromagnet is driven by a bipolar power supply setup. This setup consists of a master (KEPCO-BOP 20-20DL) and a slave (KEPCO-BOP 20-20DL) supply connected in series. The electrical DC signal is provided by a function generator (Tektronix AFG3022C). The field between the poles is measured by a hall probe that is connected to a gaussmeter (F.W.BELL 6010). The sample is held between the poles of the electromagnet by a sample holder. In order to conduct the experiment at different temperatures, the sample is placed inside a specially designed thermal chamber. The thermal chamber is fabricated of stainless steel (GRADE304) and has a thick glass wool coating on the inside and the outside to provide good thermal insulation. Temperature inside the chamber is elevated by heater rods enclosed in aluminum plates on the top and bottom of the chamber. The power input to the rods is controlled by means of a PID controller (PFU400). A K-type thermocouple is used to monitor the temperature inside the chamber. A strain gauge (FLGB-02-11,A403011,TOKYO Sokki Kenkyujo Co. Ltd.), which is glued on the surface of the sample, is connected to strain gauge indicator (SYSCON-5CH) that displays the magnetostrictive strain. Therefore, longitudinal and transverse strains are obtained. Samples used for this measurement are of dimensions of $15 \times 15 \times 1\,\text{mm}^3$. This entire setup is placed on a vibration isolation table (SANDVIC COMPONENTS) to restrict the unwanted vibrations from reaching the setup. To keep the temperature of electromagnet within safe limits, a water based cooling system in the form of a chiller is connected.

B. Fabrication of ME sample

The magnetoelectric sample comprises of three constituent parts in the form of a Ni ring, a PZT-5A ring, and a FeNi disc. Here, a Ni ring and a FeNi disc act as magnetostrictive materials, whereas the PZT-5A ceramic forms the piezoelectric part in the ME sample. Among the two magnetostrictive materials, nickel shows negative magnetostriction, whereas FeNi shows positive magnetostriction. Therefore, nickel forms the outer layer, whereas FeNi forms the inner layer of the ME sample. PZT remains sandwiched between the two magnetostrictive layers, thereby taking strain from both sides as is clear from Fig. 4(a). A press-fit nested ring structure is formed by embedding one component into the other. The dimensions of the respective samples have been provided in Table I. As is evident from the dimensions, the diameter of FeNi disc is slightly greater than the inner diameter of PZT ring, which enables it to form a tight fit by pressing it into the PZT ring. Similarly, the outer diameter of PZT ring is slightly greater than the inner diameter of nickel ring. So, FeNi/PZT assembly is pressed into the nickel ring, thus forming the ME composite. The top and the bottom face of PZT are silver plated, thereby forming two electrodes. For a comparative study, Ni/PZT and FeNi/PZT epoxy

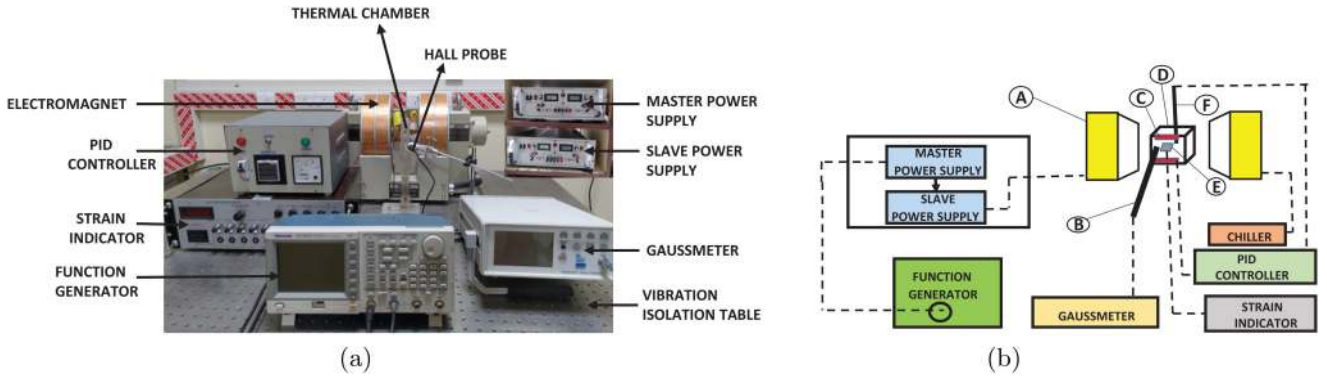

FIG. 1. (a) The experimental setup to measure magnetostriction. (b) Schematic of the experimental setup to measure magnetostriction. A: electromagnet, B: Hall probe, C: aluminum heater plate, D: thermal chamber, E: sample, F: thermocouple.

TABLE I. Sample dimensions of constituents of ring composite.

Constituent	Inner diameter (mm)	Outer diameter (mm)	Thickness (mm)
FeNi disc	…	8.05	1
PZT-5A ring	8	20.05	1
Ni ring	20	28	1

bilayered as well as Ni/PZT/Ni and FeNi/PZT/FeNi epoxy trilayered composites of similar volume fractions as of epoxy-free ring composite are prepared. These bilayered and trilayered ME composites are prepared in the conventional manner by the vacuum bagging technique in which an epoxy binds the magnetostrictive and piezoelectric layers and the composite is left in vacuum for 24 h to cure. Magnetostrictive materials (FeNi and Ni) and piezoelectric ceramics used in epoxy bonded composite have dimensions of $15 \times 15 \times 1\,\text{mm}^3$. The fabricated ring and epoxy bonded composite have been shown in Fig. 2.

C. Measurement of ME coefficient

For the measurement of the ME coefficient, a similar set up as described in the Subsection II A is used. Figure 3 shows the setup used for ME measurement along with the schematic of the same. Input signals for both the ac and dc fields are generated by the function generator. A sinusoidal AC signal at a constant frequency of 1 kHz is amplified by an amplifier (KEPCO, BOP 36-6DL). Since the voltage generated across the piezoelectric material needs to be measured, the sample electrodes are connected to a lock-in-amplifier (DSP7265). The measurement of the ME coefficient is done for epoxy-free ring composite as well as bilayered and trilayered epoxy bonded composite and a comparison is done later on.

III. FORMULATION OF THEORETICAL MODEL

This section presents the determination of the temperature dependent two dimensional hysteretic response by means of a thermodynamically consistent model including the effects of prestress. The differential of the total internal energy density function can be expressed as[32]

$$dU = TdS + \sigma_{ij}d\varepsilon_{ij} - \mu_o M_k dH_k. \tag{1}$$

Here, $\mu_o = 4\pi \times 10^{-7}$ is the permeability of free space, H_k and M_k are the components of the magnetic field vector and magnetization vector, respectively, S is the entropy and T is the absolute temperature. The expression for the total Gibb's free energy for this system is given as

$$G(\sigma_{ij}, M_k, T) = U - TS - \sigma_{ij}\varepsilon_{ij} + \mu_o M_k H_k. \tag{2}$$

Therefore, the total differential of Gibb's free energy after substitution of (1) can be written as

$$dG = -SdT - \varepsilon_{ij}d\sigma_{ij} + \mu_o H_k dM_k. \tag{3}$$

From the standard relations of thermodynamics[25] we have

$$\varepsilon_{ij} = -\frac{\partial G}{\partial \sigma_{ij}}, \quad \mu_o H_k = \frac{\partial G}{\partial M_k}. \tag{4}$$

Now, in order to obtain the relations in polynomial form we expand the above expressions in the form of a Taylor series taking variables as stress, magnetization, and temperature. The reference point for the expansion is taken as $(\sigma_{ij}, M_k, T) = (0, 0, T_r)$, where T_r is the spin reorientation temperature of the magnetostrictive material. The expansions are given as follows:

$$\begin{aligned}\varepsilon_{ij} = &-\frac{\partial^2 G}{\partial\sigma_{ij}\partial\sigma_{kl}}\sigma_{kl} - \frac{1}{2}\frac{\partial^3 G}{\partial\sigma_{ij}\partial\sigma_{kl}\partial\sigma_{mn}}\sigma_{kl}\sigma_{mn} + \cdots \\ &-\frac{1}{2}\left(\frac{\partial^3 G}{\partial\sigma_{ij}\partial M_k\partial M_l} + \frac{\partial^4 G}{\partial\sigma_{ij}\partial\sigma_{mn}\partial M_k\partial M_l}\sigma_{mn} + \cdots\right)M_k M_l \\ &-\frac{\partial^2 G}{\partial T\partial\sigma_{ij}}\Delta T - \frac{1}{2}\frac{\partial^4 G}{\partial T\partial\sigma_{ij}\partial M_k\partial M_l}\Delta T M_k M_l,\end{aligned} \tag{5}$$

$$\begin{aligned}\mu_o H_k = &\frac{\partial^2 G}{\partial M_k\partial M_l}M_l + \frac{1}{3!}\frac{\partial^4 G}{\partial M_K\partial M_i\partial M_i\partial M_j}M_l M_i M_j \\ &+\cdots+\left(\frac{\partial^3 G}{\partial\sigma_{ij}\partial M_k\partial M_l}\sigma_{ij} + \frac{1}{2}\frac{\partial^4 G}{\partial\sigma_{ij}\partial\sigma_{mn}\partial M_k\partial M_l}\sigma_{ij}\sigma_{mn} + \cdots\right)M_l \\ &+\frac{\partial^3 G}{\partial T\partial M_k\partial M_l}\Delta T M_k + \cdots + \frac{\partial^4 G}{\partial T\partial\sigma_{ij}\partial M_k\partial M_l}\Delta T\sigma_{ij}M_k.\end{aligned} \tag{6}$$

Here, $\Delta T = T - T_r$ and $T_r = 0\,^\circ\text{C}$. To enlighten the physical meaning of the partial derivatives in the above expansions, they are

FIG. 2. (a) Fabricated epoxy-free ring composite. (b) Epoxy bonded bilayered and trilayered composite.

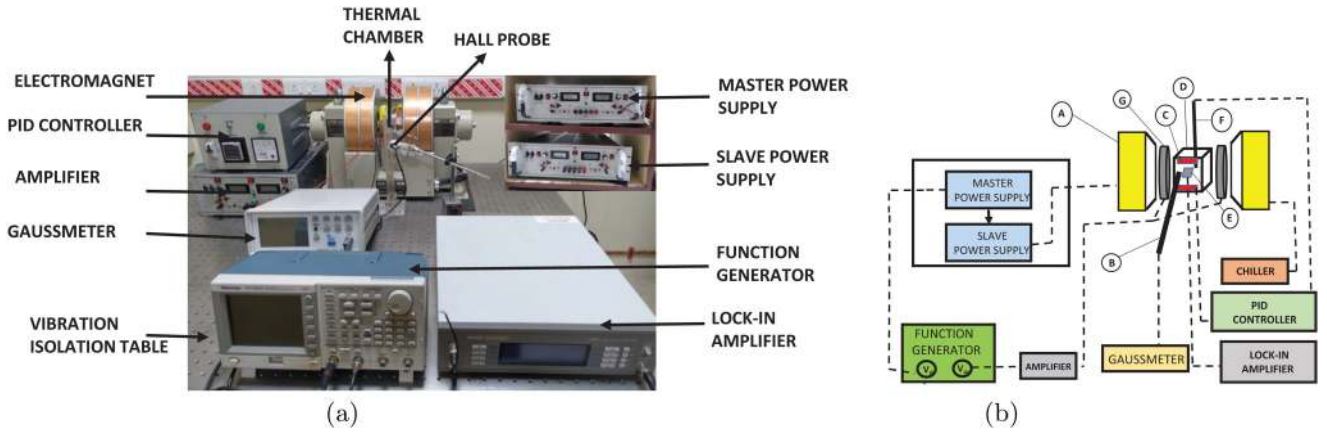

FIG. 3. (a) The experimental setup to measure ME coefficient. (b) Schematic of the experimental setup to measure ME coefficient. A: electromagnet, B: Hall probe, C: aluminum heater plate, D: thermal chamber, E: sample, F: thermocouple, G: Helmholtz coil.

written as

$$\varepsilon_{ij} = \varepsilon^0_{ij}(\sigma_{kl}) + \varepsilon^1_{ij}(M_k, \sigma_{mn}) + \alpha_{ij}\Delta T - \beta_{ij}\left(\frac{M_k}{M_s}\right)^2 \Delta T, \tag{7}$$

$$H_k = H^0_k(\sigma_{M_l}) + H^1_k(M_l, \sigma_{mn}) + \frac{2\beta_{ij}\sigma_{ij}M_k\delta T}{M_s^2}, \tag{8}$$

where each term represents their corresponding coefficients in the above expansion.

Now, in Eqs. (7) and (8), the temperature independent strain and magnetic field can be written as[27]

$$\varepsilon_{ij} = \varepsilon^0_{ij}(\sigma_{kl}) + \varepsilon^1_{ij}(M_k, \sigma_{mn}), \tag{9}$$

$$H_k = H^0_k(M_l) + H^1_k(M_l, \sigma_{mn}). \tag{10}$$

In Eq. (10), ε^0_{ij} refers to the elastic strain produced as a result of prestress. This elastic strain has two parts, one linear and the other nonlinear with respect to the stress σ_{mn}. The linear part occurs due to the conventional stress-strain interaction as for any other material and is independent of the domain wall motion. It has a linear relation with the stress σ_{mn} and is described by the use of the flexibility tensor $S^{(s)}_{ijkl}$. The nonlinear part results as the effect of the domain wall motion caused due to prestress and is represented by a nonlinear tensor function λ_{0ij}. Therefore, the elastic strain ε^0_{ij} can be expressed as

$$\varepsilon^0_{ij} = S^{(s)}_{ijkl}\sigma_{kl} + \lambda_{0ij}(\sigma_{mn}). \tag{11}$$

ε^0_{ij} is the magnetostrictive strain that is a result of magnetization owing its origin to the applied magnetic field. Therefore, it is zero in the absence of the magnetic field and reaches the maximum value when magnetization reaches saturation. $-\lambda_{0ij}(\sigma_{mn})$ should be the change in the maximum magnetostrictive strain under any prestress. In the D-H model,[25] strain has been shown to depend on the square of magnetization. Therefore, the magnetostrictive strain under a given prestress can be given as[27]

$$\varepsilon^1_{ij}(M_k, \sigma_{mn}) = \left[m_{ijkl} - \frac{\lambda_{0ij}(\sigma_{mn})}{M_s^2}\delta_{kl}\right] M_k M_l, \tag{12}$$

where the tensor m_{ijkl} is used to describe the magnetostriction in the absence of prestress. Now, the total magnetization can be decomposed into two components,[37] a reversible (linear) part and a remanent (nonlinear) part. Also, it is noteworthy that with assumption of hard and rigid magnetostrictive material, coercive field is much lower than the saturation field.[37] Thus, it can be safely assumed that the contribution of the reversible part in overall magnetization is very small with respect to the remnant part. Therefore, the model can be formulated in terms of the remnant magnetization. Therefore, from here on, magnetization and magnetic field refer to the remnant part of magnetization and magnetic field, respectively.

Magnetization curve does not follow the same path while loading and unloading, which gives rise to hysteresis. To account for this hysteresis, a yield function ϕ is assumed, which should satisfy the yield criteria analogous to the rate independent plasticity theory[8,37]

$$\phi = |\bar{H}| - H_c \leq 0. \tag{13}$$

Here, $\bar{H}$ represents

$$\bar{H} = H - H^i, \tag{14}$$

where H is the remnant part of the applied magnetic field, H^i is the internal variable analogous to back stress in the plasticity theory, H_c is the coercive field of magnetostrictive material analogous to the yield stress. A dissipation potential ψ is introduced, which corresponds to the part of free energy that is responsible for

the irreversible behavior. The internal variable in terms of dissipation potential is expressed as[8]

$$H^i = \frac{\partial \psi}{\partial M^i}, \tag{15}$$

where M^i is the remnant magnetization.

Now, the internal variable H^i is evaluated at any discrete time step t_n by assuming that the parameters corresponding to t_{n-1} are known and $M_n = M_{n-1}$.

A trial function ϕ_{trial} is assumed as follows:

$$\phi_{trial} = |H_n - H^i_{n-1}| - H_c. \tag{16}$$

If $\phi_{trial} \leq 0$, then M^i remains unchanged, while if $\phi_{trial} > 0$, then the internal variable H^i needs to be updated such that $\phi = 0$.

Since

$$\phi = |H_n - H^i_n| - H_c = |H_n - H^i_{n-1} - \Delta H^i| - H_c = 0, \tag{17}$$

ΔH^i can be evaluated as

$$\Delta H^i = |H_n - H^i_{n-1}| - H_c = \phi_{trial}. \tag{18}$$

The internal variable can be updated as follows:

$$H^i_n = H^i_{n-1} + 0.5[\phi_{trial} + |\phi_{trial}|]sign(H_n - H^i_{n-1}). \tag{19}$$

Since internal variable H^i is a function of magnetization as in (15), vice-versa will also hold true. Thus, to capture the saturation behavior of magnetization, it is expressed as a nonlinear function of the internal variable. Therefore,

$$M^i_k = f_k(H^i_l). \tag{20}$$

In Eq. (10), H^0_k represents the field corresponding to free magnetization ($\sigma_{mn} = 0$) which is given as

$$H^0_k(M^i_l) = f^{-1}_k(M^i_l). \tag{21}$$

In this work, a hyperbolic function in the form of $f(x) = \tanh(x)$ has been used as it is seen to better capture the nonlinear relationship between remnant magnetization and internal variable.

H^1_k represents the field corresponding to magnetization under the application of prestress (σ_{mn}) and can be expressed by substituting (12) in (4) as

$$\mu_o H_k = \frac{\partial G}{\partial M_k} = -\frac{\partial}{\partial M_k}\int_0^{\sigma_{ij}} \varepsilon^1_{ij}(m_k, \sigma_{mn}) d\sigma_{ij}, \tag{22}$$

$$H^1_k(M_l, \sigma_{mn}) = -2\mu_o^{-1}\left[m_{ijkl} M_l \sigma_{ij} - \frac{\Lambda_0(\sigma_{mn})}{M_s^2}\delta_{kl} M_l\right], \tag{23}$$

where $\Lambda_o = \int_0^{\sigma(mn)} \lambda_{0ij}(\sigma_{mn}) d\sigma_{ij}$.

As mentioned earlier, this model approximates remnant part of the magnetic field as the total magnetic field, thus using $H_k = H^i_k$. For low prestress levels, the nonlinear tensor function λ_{0ij} can be linearized by introducing another flexibility tensor S^m_{ijkl}.[27] Therefore, substituting (11), (12), (21), (23) in (9) and (10), the nonlinear constitutive relation is obtained as

$$\varepsilon_{ij} = S_{ijkl}\sigma_{kl} + \left[m_{ijkl} - \frac{S^{(m)}_{ijmn}\sigma_{mn}}{M_s^2}\delta_{kl}\right] M_k M_l \tag{24}$$

and

$$H^i_k = f^{-1}_k(M_l) - \mu_o^{-1}\left[2m_{ijkl}\sigma_{ij} - \frac{S^{(m)}_{ijmn}\sigma_{ij}\sigma_{mn}}{M_s^2}\right] M_l, \tag{25}$$

where

$$S_{ijkl} = S^{(s)}_{ijkl} + S^{(m)}_{ijkl}. \tag{26}$$

Now, assuming S_{ijkl} and m_{ijkl} to be the fourth order isotropic tensors, the final form of the 3D constitutive relation is obtained as follows:[27]

$$\varepsilon_{ij} = \frac{1}{E}\left[(1+\nu)\sigma_{ij} - \nu\sigma_{kk}\delta_{ij}\right] + \frac{\lambda_s}{M_s^2}\left[\frac{3}{2}M^i_i M^i_j - M^i_k M^i_k\left(\frac{1}{2}\delta_{ij} + \frac{\tilde{\sigma}_{ij}}{\sigma_s}\right)\right] + \alpha_{ij}\Delta T - \beta_{ij}\left(\frac{M_k}{M_s}\right)^2 \Delta T, \tag{27}$$

$$H^i_k = \left[\frac{1}{k(\Delta T)M^i} f^{-1}\left(\frac{M^i}{M^T_s}\right)\delta_{kl} - \frac{\lambda_s}{\mu_o M^{i2}_s}\left(2\tilde{\sigma}_{kl} - \left(I^2_\sigma - 3II_\sigma\right)\frac{\delta_{kl}}{\sigma_s}\right)\right] M^i_l + \frac{2\beta_{ij}\Delta T\sigma_{ij}M_k}{\mu_0 M_s^2}. \tag{28}$$

The above equations represent a 3D hysteretic constitutive model including the effects of prestress and temperature. In the present work, a trilayered nested ring structured ME composite has been considered. Due to symmetry, only one quadrant of the composite has been shown in Fig. 4(b) where line OO' marks the central axis of the ring composite. Now, this part of the composite can be thought of to be composed of number of strips about the central axis OO'. Sufficient number of strips are chosen such that their width is negligible and the analysis is reduced to 2D for each of the individual strips. One such strip has been shown in the figure inclined at any arbitrary angle θ with respect to the magnetic field direction. The global and the local coordinate axes has been specified. The magnetic field vector H_s can be resolved into components along the strip and in the direction of the normal to the plane of the strip as $H_x = H_s\cos\theta$ and $H_y = H_s\sin\theta$, respectively. So, the above problem is reduced to the condition of a number of strips subjected to magnetic fields in their X and Y directions.

Therefore, the above 3D constitutive relation can be reduced to a 2D relation. Also, as shown in Fig. 4, the prestress is developed in the x direction of the local coordinate axes due to the press-fit as

discussed previously. To obtain 2D expressions, the stress components out of plane are neglected, i.e., $\sigma_z = \tau_{xz} = \tau_{yz} = 0$ and unidirectional prestress condition, $\sigma_x = \sigma$, $\sigma_y = 0$, $\tau_{xy} = 0$ is imposed.

Thus, for an in-plane magnetic field (along x direction), we get

$$\begin{aligned}
\varepsilon_x &= \frac{\sigma}{E} + \frac{\lambda_s}{M_s^2}\left(1 - \frac{\sigma}{\sigma_s}\right) M_x^{i2}, \\
\varepsilon_z &= -\frac{\nu}{E}\sigma + \frac{\lambda_s}{M_s^2}\left(-\frac{1}{2} - \frac{\sigma}{2\sigma_s}\right) M_x^{i2}, \\
\gamma_{xz} &= 0, \\
H_x^i &= \frac{1}{k} f^{-1}\left(\frac{M_x^i}{M_s}\right) - \frac{\lambda_s \sigma}{\mu_o M_s^2}\left(2 - \frac{\sigma}{\sigma_s}\right) M_x^i, \\
H_z^i &= 0.
\end{aligned} \tag{29}$$

Similarly, for the field along the y direction (perpendicular to strip) relations are obtained as

$$\begin{aligned}
\varepsilon_x &= \frac{\sigma}{E} + \frac{\lambda_s}{M_s^2}\left(\frac{1}{2} - \frac{\sigma}{\sigma_s}\right) M_y^{i2}, \\
\varepsilon_z &= -\frac{\nu}{E}\sigma + \frac{\lambda_s}{M_s^2}\left(-\frac{1}{2} + \frac{\sigma}{2\sigma_s}\right) M_y^{i2}, \\
\gamma_{xz} &= 0, \\
H_y^i &= \frac{1}{k} f^{-1}\left(\frac{M_y^i}{M_s}\right) - \frac{\lambda_s \sigma}{\mu_o M_s^2}\left(-1 - \frac{\sigma}{\sigma_s}\right) M_y^i.
\end{aligned} \tag{30}$$

Equations (29) and (30) give the magnetic field and strain due to a field in along the x direction and perpendicular to the plane of the strip, respectively, without including the temperature effect.

Now, saturation magnetization is found to vary with temperature in accordance with the following relation:[29]

$$M_S^T = M_S \frac{[1 - (\Delta T + T_r + 273)/(T_C + 273)]^{1/2}}{[1 - (T_r + 273)/(T_c + 273)]^{1/2}}, \tag{31}$$

where the superscript T denotes the temperature, T_r is the spin reorientation temperature $= 0\,^{\circ}\mathrm{C}$, T_C is the Curie temperature of the magnetostrictive material. Therefore, total magnetostrictive strain in the x and z directions including the temperature effect is given as

$$\begin{aligned}
\varepsilon_x &= \frac{\lambda_s M_x^2}{M_s^2}\left(1 - \frac{\sigma}{\sigma_s}\right) - \frac{\beta \Delta T M_x^2}{M_s^2} + \frac{\lambda_s M_y^2}{M_s^2}\left(-\frac{1}{2} - \frac{\sigma}{\sigma_s}\right) - \frac{\beta \Delta T M_y^2}{M_s^2}, \\
\varepsilon_z &= \frac{\lambda_s M_x^2}{M_s^2}\left(-\frac{1}{2} - \frac{\sigma}{2\sigma_s}\right) - \frac{\beta \Delta T M_x^2}{M_s^2} + \frac{\lambda_s M_y^2}{M_s^2}\left(-\frac{1}{2} + \frac{\sigma}{2\sigma_s}\right) - \frac{\beta \Delta T M_y^2}{M_s^2}.
\end{aligned} \tag{32}$$

The remnant part of total magnetic field along x and y directions can be, respectively, given as

$$\begin{aligned}
H_x^i &= \frac{1}{k} f^{-1}\left(\frac{M_x^i}{M_s}\right) - \frac{\lambda_s \sigma}{\mu_o M_s^2}\left(2 - \frac{\sigma}{\sigma_s}\right) M_x^i - \frac{2\beta \Delta T \sigma M_x^i}{\mu_o M_s^2}, \\
H_y^i &= \frac{1}{k} f^{-1}\left(\frac{M_y^i}{M_s}\right) - \frac{\lambda_s \sigma}{\mu_o M_s^2}\left(-1 - \frac{\sigma}{\sigma_s}\right) M_y^i - \frac{2\beta \Delta T \sigma M_y^i}{\mu_o M_s^2}.
\end{aligned} \tag{33}$$

As shown in Fig. 4(a), the strain from the two magnetostrictive materials is transferred to the sandwiched piezoelectric material. But in the composite assembly, the strain of the magnetostrictive phase will not be the same as when they are free as the piezoelectric phase will offer resistance to the expansion. To account for this, a temperature dependent coefficient C_f, which is one of the model parameters, is introduced and is multiplied with the obtained free strain. Note that here free strain refers to the strain of the individual magnetostrictive material subjected to a magnetic field when they are not in the composite assembly. Thus, the total strain on the piezoelectric phase along the x and z directions is obtained. Now, the electric field generated across the thickness of the PZT strip is calculated by

$$E_z = -\frac{1}{\kappa_{33}}(e_{31}\varepsilon_x + e_{33}\varepsilon_z), \tag{34}$$

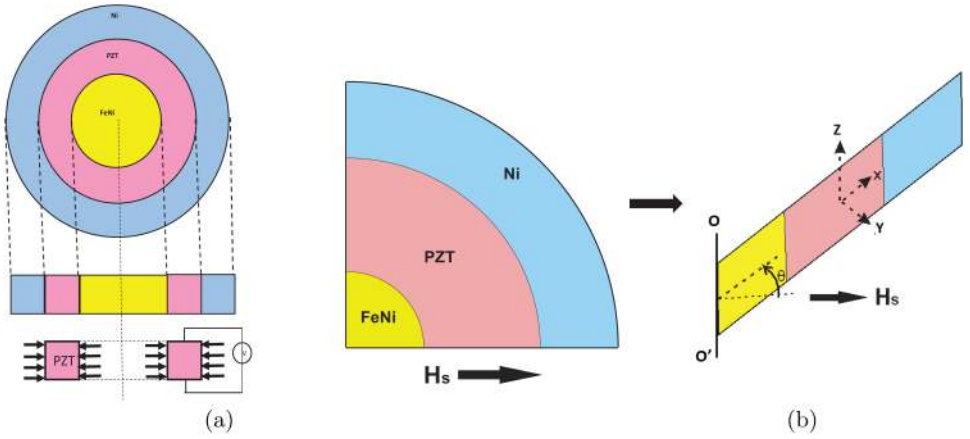

FIG. 4. (a) The schematic of the ring ME sample. (b) Schematic of the top view of a quadrant of the ring composite (since the four quadrants are symmetric); Schematic of a strip from the quadrant of the sample being subjected to magnetic field.

where κ_{33} and e_{ij} are piezoelectric coupling and strain coefficients, respectively. Once the electric field across the thickness is known, the ME coefficient can be calculated by $\alpha_{ME} = E_{ac}/H_{ac}$. The ME coefficient for all the strips are calculated and the mean value is taken, as the composite is considered to be composed of many strips as mentioned earlier. Now, since the ME composite considered shows a self-biased effect, this effect is incorporated in the model by introducing a temperature dependent model parameter C_s termed as self-biased constant, which has same dimensions as that of α_{ME}. The constant C_s is added to the obtained α_{ME} until the value of ME coefficient becomes maximum and thereafter, a loop is used to neutralize the effect of added C_s by deducting the value depending on the field as shown below

$$\alpha^{\star}_{ME} = \alpha_{ME} - \left(\frac{C_s}{H_{\alpha_0} - H_{\alpha_{\max}}}\right)(H_{current} - H_{\alpha_{\max}}). \tag{35}$$

Here, $\alpha^{\star}_{ME}$ is the updated ME coefficient, whereas H_{α_0} and $H_{\alpha_{\max}}$ are the magnetic fields at which the ME coefficient becomes zero and maximum, respectively. Therefore, as the field increases, more C_s gets deducted up to the point where it's contribution to α_{ME} becomes zero.

IV. RESULTS AND DISCUSSION

This section provides the experimental results of fabricated epoxy-free ring composites and epoxy bonded composites as well as a comparison of the simulated and experimental result.

A. Studies on magnetostriction

1. Experimental magnetostriction for Ni and FeNi

To understand the behavior of the ME composite, magnetostriction measurements were done on the individual magnetostrictive phases at different temperatures. Figures 5(a) and 5(b) show the temperature dependent longitudinal and transverse magnetostrictive strain for nickel and FeNi, respectively. The positive and negative strains in the figure depict the longitudinal and transverse strains, respectively.

It is seen that with an increase in temperature, both the longitudinal and transverse saturation magnetostrictive strain decreases for both the materials. This is because the magnetostrictive phenomenon is primarily obtained as a result of the motion of the domains in one direction and the interaction of magnetic dipoles with each other which gives rise to interaction energy.[38,39] When the temperature is increased, the thermal energy increases, thereby increasing the random motion of the domains and making it difficult for the domains to align in the direction of applied field. If the temperature is further increased, there comes a point at which the thermal energy is so high in comparison to the interaction energy that it is impossible to align the domains in one direction irrespective of the field applied. This temperature is termed as the Curie temperature. This results in a decreased value of the magnetostrictive strain at high temperatures as is evident from Fig. 5.

2. Simulated magnetostriction

Figure 6 gives the comparison of the simulation result with the experimentally obtained magnetostriction result for nickel at temperatures of 25 °C and 125 °C. The strain from the model is calculated from the expressions (32) derived in Sec. III. The material parameters for nickel used in the model are: $\chi_m = 13.33$, $M_s = 0.55T$, $\sigma_s = 220\,\text{MPa}$, $\lambda_s = 35\,\mu\text{S}$, $\beta = 0.008/^{\circ}\text{C}$, $T_C = 360\,^{\circ}\text{C}$. The strain predicted by the model is in agreement with the experimental result.

B. Studies on ME coefficient

1. ME measurement for FeNi/PZT/Ni ring composite

Measurement of the ME coefficient has been done on the fabricated epoxy-free ring composites and epoxy bonded conventional bilayered and trilayered composites. Figure 7 shows the measured ME coefficient of the epoxy-free ring composite at varying temperatures. ME response of all the measured composites of different configurations shows the conventional trend of

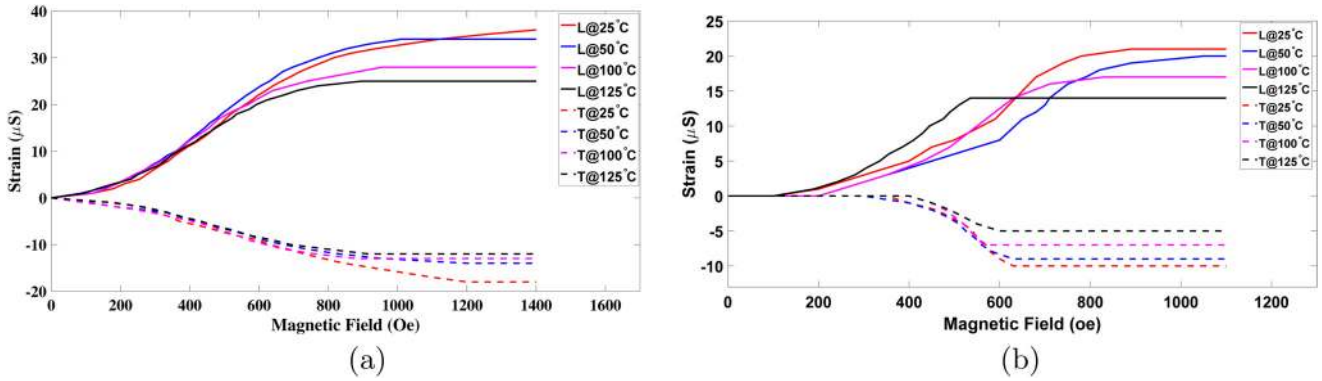

FIG. 5. (a) Magnetostriction of nickel—experimental results at 25 °C, 50 °C, 100 °C, and 125 °C. (b) Magnetostriction of FeNi—experimental results at 25 °C, 50 °C, 100 °C, and 125 °C (L: longitudinal; T: transverse).

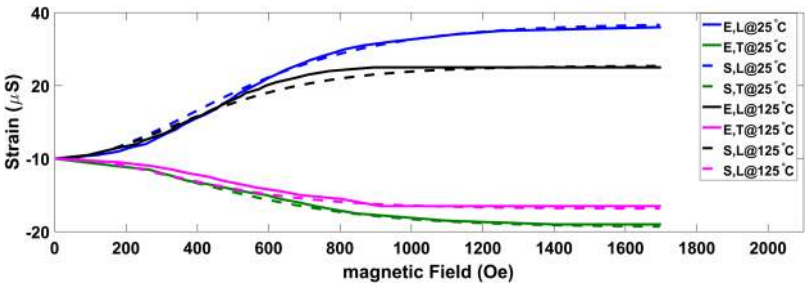

FIG. 6. Magnetostriction of nickel—experimental and simulation results at 25 °C and 125 °C. E: experimental; S: simulation; L: longitudinal; T: transverse.

first increasing, attaining a peak value and then decreasing with respect to the increasing bias field. ME coefficient α is mathematically expressed as

$$\alpha_{ME} = \frac{\partial E}{\partial H} = \left(\frac{\partial S}{\partial H}\right)\left(\frac{\partial E}{\partial S}\right). \tag{36}$$

The term $\left(\frac{\partial S}{\partial H}\right)$ in the above expression is termed as the piezomagnetic coefficient conventionally denoted as "d" and is the slope of the bias field vs magnetostriction curve. It is seen that ME coefficient is directly proportional to piezomagnetic coefficient. The dependence of piezomagnetic coefficient on the bias magnetic field for Ni at room temperature has been obtained from the magnetostriction curve and shown in Fig. 8. It is seen that the curve first increases and then decreases, which results in the similar trend for the ME coefficient. Similar reason holds true for FeNi as well. It is also seen that with an increase in temperature, the obtained ME coefficient decreases. The reason for this may be attributed to the fact that the increase in temperature leads to a decrease in magnetostrictive strain. Therefore, net strain to the PZT also decreases, which leads to decrement in the developed voltage across the electrodes giving a lower ME coefficient. Another noticeable behavior is the self-biased character of the triring composite, i.e., at zero bias field it shows a ME coefficient of 35 mV cm^{-1} Oe^{-1}. Whenever a magnetostrictive material is subjected to tensile (or compressive) stress, the domains tend to rotate in the direction parallel (or perpendicular) to the applied stress. Treating the problem analogous as that of thick wall cylinder under uniform boundary pressure,[40] it can be shown that the domains in nickel get aligned in the direction tangent to nickel ring, whereas in FeNi, they align along the thickness direction.[22] This alignment of domains leads to the generation of a magnetization which in turn is manifested in terms of strain. This strain leads to the self-biased behavior of the ring composite, which is observed only under the application of prestress.

2. ME measurement for Ni/PZT/Ni and FeNi/PZT/FeNi epoxy bonded composite

To study the relative performance of epoxy-free ring composites with conventional epoxy bonded composites at elevated temperatures, ME measurements were done on the prepared Ni/PZT/Ni and FeNi/PZT/FeNi trilayered epoxy bonded composite of similar volume fraction at different temperatures. Figures 9(a) and 9(b) show the ME coefficient of the trilayered epoxy bonded composites. For both the composites, the maximum ME coefficient is found to be around 80 mV cm^{-1} Oe^{-1}, which is similar to that obtained for the ring composite (79.5 mV cm^{-1} Oe^{-1}). Also, in the case of epoxy bonded layered composite, no self-biased character is seen as there is no prestress involved. Another observation worth mentioning is that with an increase in temperature, the performance of the epoxy bonded composites falls drastically as opposed to the epoxy-free ring composite where the performance is comparatively very good even at elevated temperatures (40 mV cm^{-1} Oe^{-1} at 125 °C). This can be attributed to the fact that in epoxy bonded

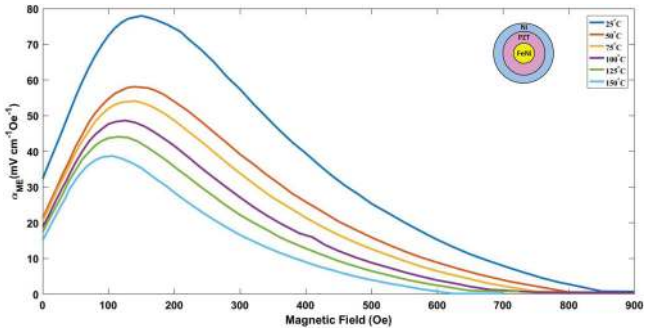

FIG. 7. Magnetoelectric coefficient of FeNi/PZT/Ni ring composite at 25 °C, 50 °C, 75 °C, 100 °C, 125 °C, and 150 °C.

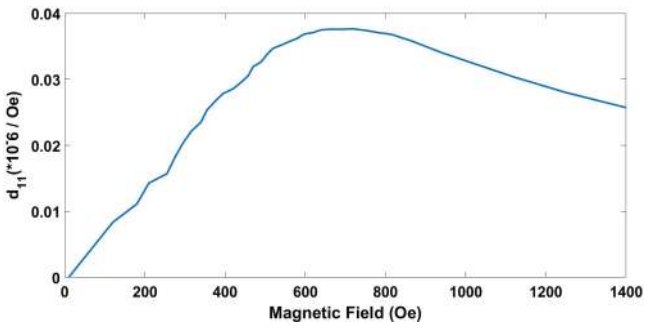

FIG. 8. Magnetic field dependence of piezomagnetic coefficient d_{11} for Ni at room temperature.

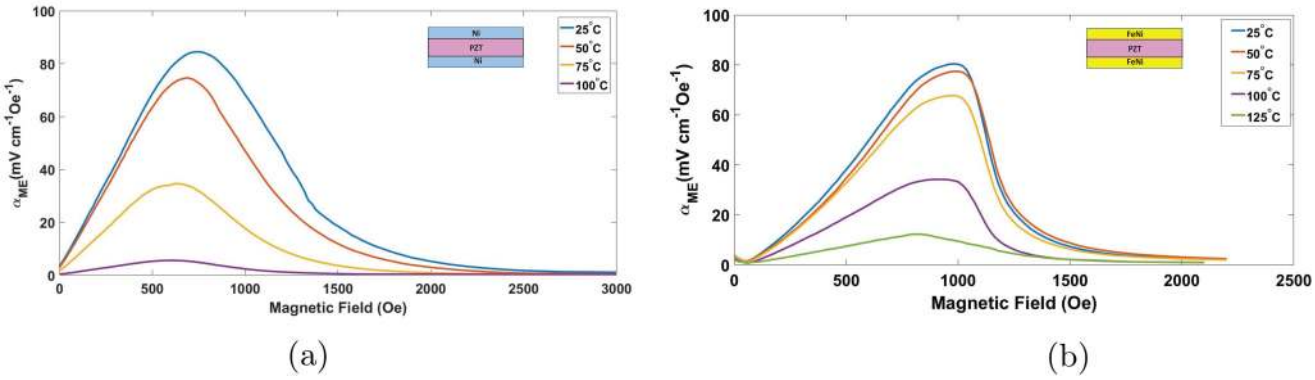

FIG. 9. (a) α_{ME} for Ni/PZT/Ni trilayered epoxy bonded composite at different temperatures. (b) α_{ME} for FeNi/PZT/FeNi trilayered epoxy bonded composite at different temperatures.

composites, the obtained ME coefficient is largely dependent on the properties of the epoxy, which acts as the medium of strain transfer from the magnetostrictive to the piezoelectric phase. At higher temperatures, the properties of the epoxy degrade drastically, thereby leading to a decreased strain transfer resulting in the fall of the obtained ME coefficient. This also explains the reason behind the ring composites displaying appreciable self-biased characteristic even at elevated temperatures (18 mV cm^{-1} Oe^{-1} at 125 °C), which makes their use feasible in high temperature microdevices.

3. ME measurement for Ni/PZT and FeNi/PZT ring composite

In order to determine the effectiveness of trilayered composites as opposed to bilayered ones, Ni/PZT and FeNi/PZT ring composites with similar volume fractions of the magnetostrictive and piezoelectric material as in trilayered composites are fabricated and ME measurements are done. Figures 10(a) and 10(b) show the obtained experimental results for Ni/PZT and FeNi/PZT ring composite, respectively. The maximum ME coefficient measured at room temperature measured for Ni/PZT ring composite is 62 mV cm^{-1} Oe^{-1}, which is around 20% less than that measured for triphase ring composites. Self-biased character also gets decreased by about 15%. This fall in value may be because of the absence of the inner magnetostrictive material, which leads to the strain transfer to PZT only from one of the faces (on the outer diameter). Similar measurements on FeNi/PZT ring composite show a maximum value of 24 mV cm^{-1} Oe^{-1}. This decrement could be because FeNi gives less magnetostrictive strain than Ni. The self-biased character in FeNi/PZT ring composite is significantly reduced because as discussed earlier, prestress causes the domains in FeNi to align along the thickness of the sample, thereby generating the internal field along thickness direction. Therefore, the strain also occurs in the same direction and thus the strain transfer from FeNi to PZT is parallel to the contact surface (along the contact surface in thickness direction). Therefore, this leads to a low strain transfer, which results in a significant decrease in the self-biased nature of the composite.

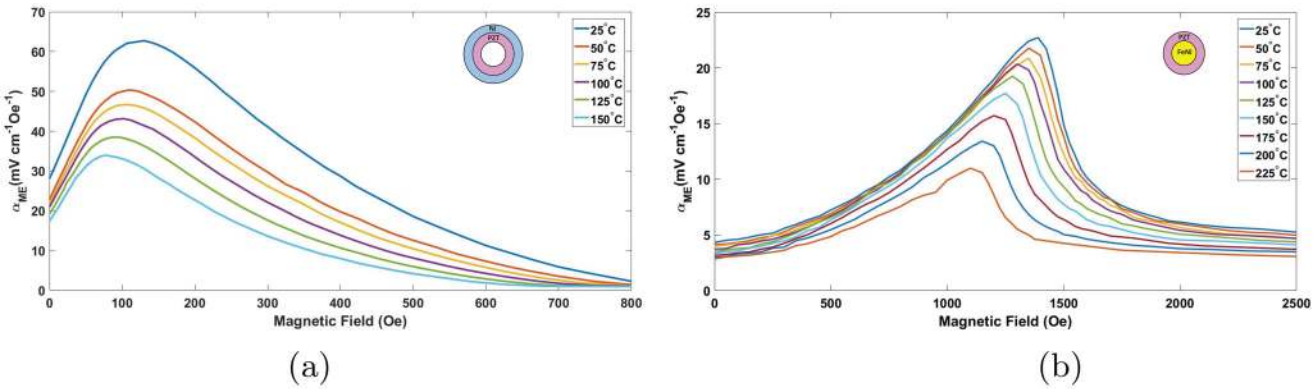

FIG. 10. (a) α_{ME} for Ni/PZT epoxy-free ring composite at different temperatures. (b) α_{ME} for FeNi/PZT epoxy-free ring composite at different temperatures.

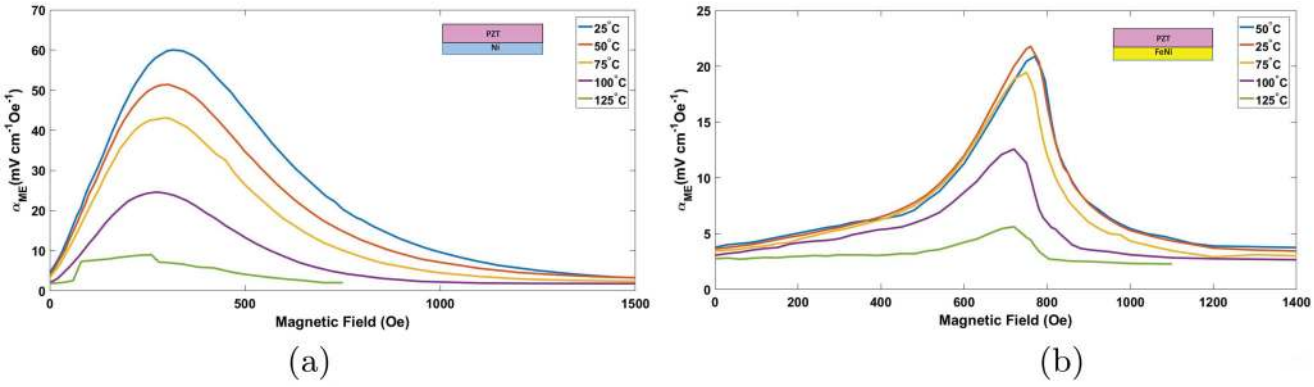

FIG. 11. (a) α_{ME} for Ni/PZT epoxy bonded layered composite at different temperatures. (b) α_{ME} for FeNi/PZT epoxy bonded layered composite at different temperatures.

4. ME measurement for Ni/PZT and FeNi/PZT epoxy bonded composite

The results for two phase ring composites were further compared with epoxy bonded Ni/PZT and FeNi/PZT bilayered composites of similar individual volume fractions. Figures 11(a) and 11(b) show the measured value of ME coefficient for Ni/PZT and FeNi/PZT epoxy bonded bilayered composites, respectively. As is observed from the plot 11(a), the maximum ME coefficient for Ni/PZT epoxy composite is slightly less than that of Ni/PZT ring composite at room temperature. When the temperature is increased, there is a rapid fall in the value of ME coefficient and at 150 °C epoxy composite gives a maximum of 8 mV cm^{-1} Oe^{-1} as opposed to 34 mV cm^{-1} Oe^{-1} obtained in the case of similar ring composite. Similarly, for FeNi/PZT epoxy composite, the maximum value of ME coefficient at room temperature is 23 mV cm^{-1} Oe^{-1}, which is nearly same as obtained for FeNi/PZT ring composite but with increase in temperature the decrement in case of epoxy composite is very high as compared to ring composite. At 125 °C, the decrement in the value for epoxy composite is nearly 77%, whereas for epoxy-free ring composite the decrement is only 15%. The reason for this can directly be attributed to the degraded properties of epoxy at elevated temperatures as discussed earlier. Since the prestress is absent in case of epoxy bonded composites, negligible self-biased behavior is observed. A point worth mentioning is that even at temperatures as high as 225 °C, ring composites performs fairly well and gives a maximum ME coefficient of around 11 mV cm^{-1} Oe^{-1} whereas in case of epoxy bonded composites it becomes difficult to realize the ME coefficient even at temperatures of 125 °C.

Another notable observation is the manifestation of the peak of ME response at different bias fields for different configurations. Table II provides the bias magnetic fields at which samples of different configurations show the maximum value of the ME coefficient at room temperature.

The bias field required for attaining maximum ME response in the case of Ni/PZT/FeNi and Ni/PZT ring composite is considerably low as compared to any other configuration. This may be attributed to the effect of prestress, which imparts a considerable degree of magnetization in the material without the application of any bias field. However, this is not manifested significantly in FeNi/PZT ring composite as the domains align in the transverse direction as discussed earlier in Sec. IV B 1 and, therefore, a lower field is required for the switching of the remaining domains.

Thus, from the above results, it is seen that at room temperature, the performance of the fabricated epoxy-free ring composite is equivalent and even better in some cases as compared to epoxy bonded composites. At elevated temperatures, the performance of ring composite is much better as compared to epoxy bonded composites. Also, with the presence of prestress, the ring composite shows considerable self-biased behavior even at high temperatures making its use possible in high temperature microdevices, whereas no such behavior is seen in the case of epoxy bonded composites due to the absence of prestress.

5. Simulated ME coefficient for FeNi/PZT/Ni ring composite

A 2D hysteretic model capturing the effects of temperature and prestress has been developed to predict the behavior of the ring structured ME composite at a given temperature. Same properties of nickel as mentioned before in Sec. IV A 2 has been used. The properties of FeNi that has been used are given as: $\chi_m = 10$, $M_s = 1.179$ T, $\sigma_s = 220$ MPa, $\lambda_s = 21\,\mu$S, $\beta = 0.007/^\circ$C,

TABLE II. Bias fields corresponding to maximum ME response.

Sample configuration	Bias field at maximum α_{ME}
Ni/PZT/FeNi ring	150
Ni/PZT/Ni trilayered epoxy	750
FeNi/PZT/FeNi trilayered epoxy	970
Ni/PZT ring	130
FeNi/PZT ring	1390
Ni/PZT bilayered epoxy	315
FeNi/PZT bilayered epoxy	770

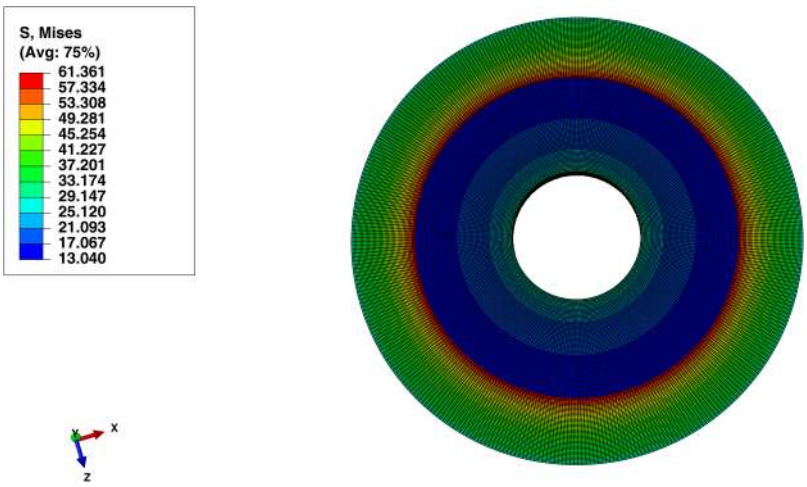

FIG. 12. ABAQUS results for the prestress developed at the Ni/PZT interface of the FeNi/PZT/Ni ring composite.

$T_C = 510\,^{\circ}\mathrm{C}$. The material properties for piezoelectric material at room temperature has been taken as $\kappa_{33} = 16.4 \times 10^{-9}\,\mathrm{C^2/N\,m^2}$, $e_{31} = -4.235\,\mathrm{C/m^2}$, $e_{33} = 21.94\,\mathrm{C/m^2}$, where κ_{ij} and e_{ij} are the piezoelectric coupling and strain coefficients, respectively. Since the properties of the piezoelectric material vary with variations in temperature, the above properties at higher temperatures have been taken from Ref. 41. It is evident from the experimental results that the prestress developed at the Ni/PZT interface plays a vital role in the obtained behavior of the ring composite. In order to determine this prestress, the Ni/PZT ring structure of similar dimensions as used in experiment has been simulated in ABAQUS, the results of which have been shown in Fig. 12. From the simulated result, the value of prestress considered in the model is 61 MPa.

Figure 13 presents the simulation results from the model and their comparison with the experimental results for FeNi/PZT/Ni ring composite at temperatures of 25 °C, 75 °C, and 150 °C. The model is able to successfully predict the experimental results at all the given temperatures with slight deviations at high fields.

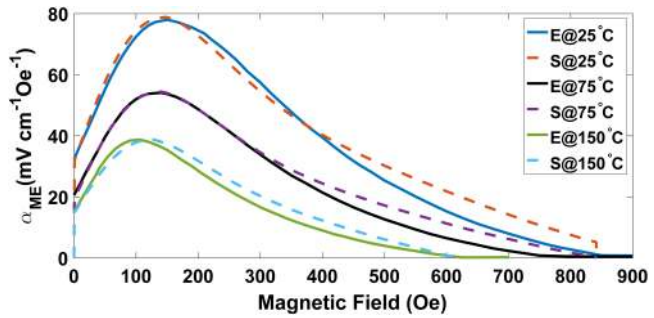

FIG. 13. Experiment vs simulation ME coefficient for the FeNi/PZT/Ni ring composite at 25 °C, 75 °C, and 150 °C (frequency of ac signal = 1 kHz). E: experiment; S: simulation.

V. CONCLUSION

Press-fit epoxy-free nested ring structured FeNi/PZT/Ni, FeNi/PZT, and Ni/PZT ME composites have been fabricated. For a comparative study, conventional epoxy bonded trilayered Ni/PZT/Ni and FeNi/PZT/FeNi along with bilayered FeNi/PZT and Ni/PZT ME composites have also been prepared. Magnetostriction measurements on individual magnetostrictive components and ME measurements on the above mentioned ME composites at various temperatures are done. A thermodynamically consistent 2D hysteretic model taking into account the effects of prestress and temperature has been developed to predict the behavior of the epoxy-free triring composite. The major observations from the experiments and simulation are:

(a) For individual magnetostrictive materials (Ni and FeNi), saturation longitudinal and transverse magnetostrictive strains decrease as the temperature is increased. The developed model is able to predict the magnetostrictive strain at different temperatures.

(b) At room temperature, the performance of epoxy-free ring composites is either equivalent or in some cases better than that of epoxy bonded composites of similar material constituents with similar volume fractions of the magnetostrictive and piezoelectric material. The performance of nickel based composites are better than FeNi based composites.

(c) The ME coefficient decreases with an increase in temperature for fabricated epoxy-free ring and epoxy bonded layered composite but the decrement in the case of the ring composite is much less as compared to that of epoxy bonded composites.

(d) Ring composites are found to show reasonable self-biased behavior, which is not observed in epoxy bonded layered composites.

(e) Unlike epoxy bonded composites, ring composites show good ME response and self-biased character even at temperatures above 150 °C, which makes their use feasible in high temperature microdevices.

(f) The developed composite model is able to predict the behavior of the epoxy-free FeNi/PZT/Ni triring composite at varying temperatures with slight deviations at higher fields.

At the present state of art, the practical applicability of the epoxy-free ring composite is not as wide as compared to the conventional layered composite but the advantages they offer over conventional counterparts, especially under thermal environment, motivates the research in this regard. With the development of better and uniform fabrication techniques, the epoxy-free ring composite is expected to show a better ME response as compared to the epoxy bonded composite.

ACKNOWLEDGMENTS

This work is financially assisted by the Science and Engineering Research Board (SERB), DST, India, under Project No. EMR/2015/001559. The authors would like to extend their gratitude to the Defence Metallurgical Research Laboratory (DMRL) Hyderabad, India and Defence Research and Development Organisation (DRDO), India, under ER&IPR scheme (Project No. ERIP/ER/201612008/M/01/1713). The authors gratefully acknowledge Dr. J. Arout Chelvane, DMRL, India, for the effective technical discussions.

REFERENCES

[1]C.-W. Nan, M. Bichurin, S. Dong, D. Viehland, and G. Srinivasan, J. Appl. Phys. **103**, 031101 (2008).
[2]C. M. Leung, J. Li, D. Viehland, and X. Zhuang, J. Phys. D Appl. Phys. **51**, 263002 (2018).
[3]Z. Chu, M. PourhosseiniAsl, and S. Dong, J. Phys. D Appl. Phys. **51**, 243001 (2018).
[4]H. Palneedi, V. Annapureddy, S. Priya, and J. Ryu, in *Actuators* (Multidisciplinary Digital Publishing Institute, 2016), Vol. 5, p. 9.
[5]M. Bichurin, V. Petrov, S. Priya, and A. Bhalla, Adv. Condens. Matter Phys. **2012**, 129794 (2012).
[6]M. Paluszek, D. Avirovik, Y. Zhou, S. Kundu, A. Chopra, R. Montague, and S. Priya, in *Composite Magnetoelectrics*, edited by G. Srinivasan, S. Priya, and N. X. Sun (Woodhead Publishing, 2015), pp. 297–327.
[7]J. Wan, J.-M. Liu, H. Chand, C. Choy, G. Wang, and C. Nan, J. Appl. Phys. **93**, 9916 (2003).
[8]S. M. Subhani, S. Maniprakash, and A. Arockiarajan, Acta Mech. **228**, 3185 (2017).
[9]S. Mandal, G. Sreenivasulu, V. Petrov, and G. Srinivasan, Phys. Rev. B **84**, 014432 (2011).
[10]S. Mandal, G. Sreenivasulu, V. Petrov, and G. Srinivasan, Appl. Phys. Lett. **96**, 192502 (2010).
[11]J. Zhang, D. Chen, K. Li, D. Filippov, B. Ge, Q. Zhang, X. Hang, L. Cao, and G. Srinivasan, AIP Adv. **9**, 035137 (2019).
[12]J. Ma, C. Xin, J. Ma, Y. Lin, and C. Nan, AIP Adv. **7**, 035013 (2017).
[13]Y. Zhou, S. Chul Yang, D. J. Apo, D. Maurya, and S. Priya, Appl. Phys. Lett. **101**, 232905 (2012).
[14]J. Zhang, P. Li, Y. Wen, W. He, A. Yang, D. Wang, C. Yang, and C. Lu, Appl. Phys. Lett. **105**, 172408 (2014).
[15]J. Zhang, P. Li, Y. Wen, W. He, A. Yang, and C. Lu, Appl. Phys. Lett. **103**, 202902 (2013).
[16]S.-C. Yang, C.-S. Park, K.-H. Cho, and S. Priya, J. Appl. Phys. **108**, 093706 (2010).
[17]Y. Wang, Y. Su, J. Li, and G. J. Weng, J. Appl. Phys. **117**, 164106 (2015).
[18]Y. Wang, X. Xia, and G. J. Weng, Rev. Adv. Mater. Sci. **48**, 78 (2017).
[19]Y. Yan, Y. Zhou, and S. Priya, Appl. Phys. Lett. **102**, 052907 (2013).
[20]D. Pan, Y. Bai, W. Chu, and L. Qiao, J. Phys. D Appl. Phys. **41**, 022002 (2007).
[21]D. Pan, Y. Bai, A. A. Volinsky, W. Chu, and L. Qiao, Appl. Phys. Lett. **92**, 052904 (2008).
[22]W. Jing and F. Fang, Appl. Phys. Lett. **106**, 212901 (2015).
[23]G. P. Carman and M. Mitrovic, J. Intell. Mater. Syst. Struct. **6**, 673 (1995).
[24]M. B. Moffett, A. E. Clark, M. Wun-Fogle, J. Linberg, J. P. Teter, and E. A. McLaughlin, J. Acoust. Soc. Am. **89**, 1448 (1991).
[25]T. Duenas, L. Hsu, and G. Cakman, MRS Online Proc. Library Archive **459**, 527–543 (1996).
[26]Y. Wan, D. Fang, and K.-C. Hwang, Int. J. Non-Linear Mech. **38**, 1053 (2003).
[27]X. Zheng *et al.*, Acta Mech. Sin. **21**, 278 (2005).
[28]X. Zheng and X. Liu, J. Appl. Phys. **97**, 053901 (2005).
[29]X. J. Zheng and L. Sun, J. Appl. Phys. **100**, 063906 (2006).
[30]H.-M. Zhou, Y.-H. Zhou, and X.-J. Zheng, J. Appl. Phys. **104**, 023907 (2008).
[31]K. Linnemann, S. Klinkel, and W. Wagner, Int. J. Solids Struct. **46**, 1149 (2009).
[32]T.-Z. Wang and Y.-H. Zhou, J. Appl. Phys. **108**, 123905 (2010).
[33]L. Wang, B.-W. Wang, Z.-H. Wang, L. Weng, W.-M. Huang, and Y. Zhou, Rare Metals **32**, 486 (2013).
[34]D.-G. Zhang, M.-H. Li, and H.-M. Zhou, AIP Adv. **5**, 107201 (2015).
[35]Y. Xiao, X.-F. Gou, and D.-G. Zhang, J. Magn. Magn. Mater. **441**, 642 (2017).
[36]G. Liu, C.-W. Nan, N. Cai, and Y. Lin, Int. J. Solids Struct. **41**, 4423 (2004).
[37]D. Fang, X. Feng, and K. Hwang, Proc. Inst. Mech. Eng. C **218**, 1405 (2004).
[38]J. Schröder and D. C. Lupascu, in *Ferroic Functional Materials: Experiment, Modeling and Simulation* (Springer, 2017), Vol. 581.
[39]W. K. Panofsky and M. Phillips, *Classical Electricity and Magnetism* (Courier Corporation, 2005).
[40]S. Timoshenko and J. Goodier, *Theory of Elasticity* (Mcgraw Hill, New York, 1951).
[41]M. Hooker, Technical Report, CR-1998-208708, 1998.